How to cite: *Angew. Chem. Int. Ed.* **2022,** *61,* e202114902
International Edition: doi.org/10.1002/anie.202114902
German Edition: doi.org/10.1002/ange.202114902

VIP **Solid-State Chemistry** **Very Important Paper**

Nitridic Analogs of Micas $AESi_3P_4N_{10}(NH)_2$ (AE = Mg, $Mg_{0.94}Ca_{0.06}$, Ca, Sr)

Lucien Eisenburger, Philipp Strobel, Peter J. Schmidt, Thomas Bräuniger, Jonathan Wright, Eleanor Lawrence Bright, Carlotta Giacobbe, Oliver Oeckler, and Wolfgang Schnick**

Abstract: *We present the first nitridic analogs of micas, namely $AESi_3P_4N_{10}(NH)_2$ (AE = Mg, $Mg_{0.94}Ca_{0.06}$, Ca, Sr), which were synthesized under high-pressure high-temperature conditions at 1400 °C and 8 GPa from the refractory nitrides P_3N_5 and Si_3N_4, the respective alkaline earth amides, implementing NH_4F as a mineralizer. The crystal structure was elucidated by single-crystal diffraction with microfocused synchrotron radiation, energy-dispersive X-ray spectroscopic (EDX) mapping with atomic resolution, powder X-ray diffraction, and solid-state NMR. The structures consist of typical tetrahedra–octahedra–tetrahedra (T-O-T) layers with P occupying T and Si occupying O layers, realizing the rare motif of sixfold coordinated silicon atoms in nitrides. The presence of H, as an imide group forming the $SiN_4(NH)_2$ octahedra, is confirmed by SCXRD, MAS-NMR, and IR spectroscopy. Eu^{2+}-doped samples show tunable narrow-band emission from deep blue to cyan (451–492 nm).*

Silicates offer a broad range of structural diversity ranging from discrete SiO_4 tetrahedra to ribbons, sheets and frameworks. These structural motifs are unmatched in their diversity as compared to other tetrahedral anions like phosphates, sulfates or vanadates. Such structural diversity accompanied by chemical stability and their mechanical properties allows silicates to be employed in several applications, e.g. dielectrics, construction materials, fire retardants, and as host compounds for activator ions in luminescent materials.[1–3] The plethora of structural motifs is enabled by the feasibility of SiO_4 tetrahedra to condense in a manifold of patterns. Whereas oxygen atoms rarely interconnect more than two tetrahedra, in silicate-related structures, nitrogen atoms may even bridge up to four tetrahedra, which for example form star-shaped units and even edge-sharing tetrahedra have been observed. This has led to a multitude of compounds with very diverse structures. The manifold of structures has also been observed when tetrahedra centers were exchanged for P in so-called nitridophosphates. Many of these compounds exhibit promising properties for application in phosphor-converted LEDs.[4,5] Structural diversification can be furthermore enhanced by mixed networks in terms of oxo- and nitridosilicates alike as displayed by alumosilicates and their related nitridoalumosilicates.

Syntheses of nitridosilicates and -phosphates are typically performed at high temperatures (>1000 °C) and, especially for nitriodophosphates often under high pressures (>4 GPa).[6] With the recent discovery of SiP_2N_4NH, a significant step was taken to accommodate the high-pressure motif of SiN_6 octahedra.[7–9] Sixfold coordinated Si atoms are also very rare in oxidic compounds where examples include rutile-type stishovite, a high-pressure polymorph of SiO_2, or $K_2Si[Si_3O_9]$.[10,11] Despite the aforementioned structural diversity, the observation of mineral-analogous nitridosilicates and -phosphates is uncommon if the charge of the counterion is to be preserved. This is simply explained by the high anionic charge of the nitride networks. The incorporation of Si and P allows mitigating the high anionic charge thus enabling the syntheses of mineral analogous compounds like $AESiP_3N_7$ (AE = Sr, Ba), which crystallize isotypic to the mineral barylite ($BaBe_2Si_2O_7$).[12] Synthetic challenges targeting nitridosilicate phosphates arise from the decomposition of P_3N_5 at temperatures above 850 °C and the relative chemical inertness of Si_3N_4. This problem has been overcome by high partial pressures of HCl (SiP_2N_4NH) or employing small amounts of NH_4F ($AESiP_3N_7$ (AE = Sr, Ba)) as mineralizing agents and applying high external pressures of 8 GPa at 1100–1700 °C realized by a multianvil press.[7,12] As shown previously, NH_4F seems to be able to reversibly cleave the bonds in refractory nitrides allowing straightforward synthesis of nitridic compounds.[12,13] NH_4F however cannot be found in the reaction products as side reactions with the BN crucible material seem possible.

[*] L. Eisenburger, Dr. T. Bräuniger, Prof. Dr. W. Schnick
Department of Chemistry, University of Munich
Butenandtstraße 5–13, 81377 Munich (Germany)
E-mail: wolfgang.schnick@uni-muenchen.de
Dr. P. Strobel, Dr. P. J. Schmidt
Lumileds Phosphor Center Aachen (LPCA)
Lumileds (Germany) GmbH
Philipsstraße 8, 52068 Aachen (Germany)
Dr. J. Wright, Dr. E. L. Bright, Dr. C. Giacobbe
ESRF, The European Synchrotron
71 Avenue des Martyrs, CS40220, 38043 Grenoble Cedex 9 (France)
Prof. Dr. O. Oeckler
Institute for Mineralogy, Crystallography and Materials Science
Leipzig University
Scharnhorststraße 20, 04275 Leipzig (Germany)
E-mail: oliver.oeckler@gmx.de

Following the NH_4F mineralizer-assisted approach we have now found a simple way to access mica-like layered imidonitridosiliconphosphates $AESi_3P_4N_{10}(NH)_2$ (AE = Mg, $Mg_{0.94}Ca_{0.06}$, Ca, Sr) at high-pressure/high-temperature conditions (details are described in Ref. [14]) from the respective AE-amide, P_3N_5, and Si_3N_4 with NH_4F as a mineralizer according to Equation (1). To further investigate luminescence properties, Eu^{2+}-doped samples have been synthesized by addition of ≈1 mole% of EuF_3 (with respect to AE) to the starting mixtures.

$$3\,AE(NH_2)_2 + 4\,P_3N_5 + 3\,Si_3N_4 \rightarrow 3\,AESi_3P_4N_{10}(NH)_2 + 2\,NH_3 \quad (1)$$

The reactions yielded the title compounds as colorless, microcrystalline powders, which are stable towards air and moisture. Samples of $AESi_3P_4N_{10}(NH)_2$ (AE = $Mg_{0.94}Ca_{0.06}$, Ca, Sr) doped with Eu^{2+} are yellow. More details on the synthesis are given in the Supporting Information. The crystal structure of $CaSi_3P_4N_{10}(NH)_2$, was elucidated by single-crystal diffraction (SCXRD) with microfocused synchrotron radiation ($C2/m$ (no. 12), a = 4.91790(10), b = 8.5159(2), c = 9.8267(2) Å, β = 99.476(3)°, Z = 2, R_1 = 0.0805). For this purpose, pre-characterized crystallites on TEM-grids (Figure S1) were used at beamline ID11 of the ESRF (Grenoble, France).[15–17] Data from two twinned crystallites were merged to increase completeness. Structure elucidation from single-crystal X-ray diffraction (SCXRD) enabled Rietveld refinements, also for the compounds with AE = Mg, $Mg_{0.94}Ca_{0.06}$, and Sr. The imidonitridosiliconphosphates $AESi_3P_4N_{10}(NH)_2$ are isotypic to e.g. clintonite, a brittle mica with composition $Ca(Mg,Al)_3(Al_3Si)O_{10}(OH)_2$.[18] Single-crystal diffraction patterns of $CaSi_3P_4N_{10}(NH)_2$ show diffuse streaks and signs of twinning, which are typical for mica-type materials.[19,20] Twinning by rotation of 120° around [310] for both crystals was taken into account and the position of H was determined from difference Fourier maps. The N–H bond length was restrained at 0.89 Å.[21]

Elemental compositions of the title compounds were confirmed by X-ray spectroscopy (EDX) (Table S6) and phase compositions of respective samples were analyzed by Rietveld refinements (Figures S2–S5, Tables S7–S11). The structures of $AESi_3P_4N_{10}(NH)_2$ (AE = Mg, $Mg_{0.9}Ca_{0.1}$, Ca, Sr) consist of layers of AEN_6 octahedra, PN_4 tetrahedra and $SiN_4(NH)_2$ octahedra following the general scheme of tetrahedra–octahedra–tetrahedra (*T*-*O*-*T*) arrangement for mica-like structures (Figure 1).[22,23]

Interatomic distances P–N range from 1.614(6) to 1.702(5) Å with the latter corresponding to a surprisingly long P–N bond that is comparable to those in compounds like $Sr_3P_3N_7$ (1.683(11) Å), Mg_2PN_3 (1.693(5) Å) and β-HP_4N_7 (1.697(2) Å).[21,24,25] Bond lengths Si–N range between 1.837(8) and 1.923(7) Å; similar to those reported for the high-pressure compounds γ-Si_3N_4 (1.8626(1) Å) or SiP_2N_4NH (1.8031(9)–2.0146(10) Å).[7–9]

The title compounds incorporate the alkaline earth metals Mg, Ca and Sr, which results in the lattice parameter c varying by ≈0.8 Å. Synthesis aiming at $BaSi_3P_4N_{10}(NH)_2$, however, yielded $BaSiP_3N_7$. Possibly, Ba cannot be accommodated, which can be explained by the limited space along [100] and [010] compared with micas with high Ba-content like kinoshitalite ($BaMg_3[Al_2Si_2O_{10}](OH)_2$).[26]

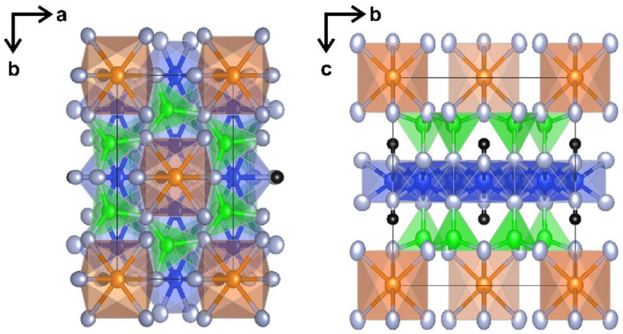

Figure 1. Structure of $CaSi_3P_4N_{10}(NH)_2$ with coordination polyhedra of Ca displayed in orange, P green, Si blue, N gray and H black. Displacement ellipsoids are displayed with 99% probability (except for H).

As the correct assignment of atom types to crystallographic positions is impeded by the similar X-ray scattering form factors of Si and P, STEM-EDX mappings with atomic resolution were performed (Figure 2). The overlay of STEM-EDX maps with an HAADF image shows the ordering of Si and P and led to the conclusion that the title compounds consist of PN_4 tetrahedra and $SiN_4(NH)_2$ octahedra.

IR spectra (Figure S17) show absorption bands for each of the title compounds at 3313–3334 cm^{-1}, indicating the presence of N–H stretching vibrations.[27] The positions of

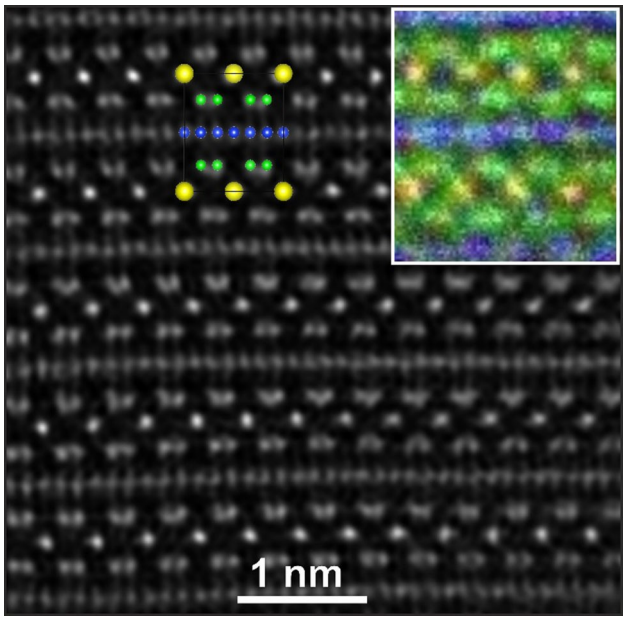

Figure 2. STEM HAADF image of $CaSi_3P_4N_{10}(NH)_2$ along [100] with structure projection (top middle) and EDX map top right. Ca yellow, P green and Si blue. H and N were omitted for clarity. Further experimental details are given in the Supporting Information.

the corresponding H atom were localized from single-crystal diffraction data and confirmed by solid-state NMR as imide groups adjacent to Si, forming $SiN_4(NH)_2$ octahedra.

All signals in ^1H, ^{31}P, cross-polarized (CP) $^1H\rightarrow^{31}P$ and $^1H\rightarrow^{29}Si$ (indicated by the notation {1H}) $^{31}P\{1H\}$ and $^{29}Si\{1H\}$ MAS NMR spectra of $CaSi_3P_4N_{10}(NH)_2$ shown in Figure 3 are consistent with the structure model. Additional weak peaks are attributed to the side phase $MgSi_3P_4N_{10}(NH)_2$, which forms by reaction with MgO spacer disks used in the multianvil assembly. The sharp ^{31}P signal at 3.5 ppm corresponds to the single Wyckoff site and agrees with NMR data for P in SiP_2N_4NH. The persistence of this signal in the $^{31}P\{1H\}$ measurements indicates the vicinity of H to the P site. $^{29}Si\{1H\}$ spectra show two signals with an estimated integral ratio of 1:2 centered at 214.6 and 215.6 ppm, respectively. Although the use of integrated intensities is problematic for CP spectra, it is warranted here in good approximation as the average distances of the ^{29}Si to the four neighboring protons in the structure are similar, see Table S13. The two ^{29}Si resonances can accordingly be attributed to the Wyckoff sites 2*d* and 4*h* occupied by sixfold coordinated Si, comparable to γ-Si_3N_4 and SiP_2N_4NH with resonances at −225 and −205 ppm, respectively.[7,28] Again, the presence of both signals in cross-polarization experiments indicates the vicinity of H to both Si sites. ^1H NMR shows a strong signal at 6.8 ppm, consistent with H localized above the $SiN_4(NH)_2$ layers and centered in the void formed by the PN_4 *sechser* rings. BVS calculations (Table S14) are in agreement with the structure model.[29]

The thermal behavior of $CaSi_3P_4N_{10}(NH)_2$ was analyzed by temperature-dependent powder X-ray diffraction (PXRD), revealing thermal stability up to 900 °C with exceptionally low thermal expansion of the unit cell volume (Figure S10–S12).

The direct optical band gaps of the undoped title compounds derived from Tauc plots amount to 4.6, 4.2 and 3.9 eV for AE = Mg, Ca, Sr, respectively, with decreasing band gap towards heavier homologs (Figure S18).[30,31] The large band gaps are beneficial concerning luminescence of Eu^{2+}-doped samples. The only reported luminescent imidonitride so far is $BaP_6N_{10}NH:Eu^{2+}$ with λ_{max} = 451 nm and a FWHM of 52 nm (2423 cm^{-1}).[32] $SrSi_3P_4N_{10}(NH)_2:Eu^{2+}$ and $CaSi_3P_4N_{10}(NH)_2:Eu^{2+}$ show narrow emission bands upon excitation with UV light at λ_{max} = 451 nm and 478 nm with FWHMs of 26 nm (1300 cm^{-1}) and 30 nm (1298 cm^{-1}), respectively (Figure 4).

$MgSi_3P_4N_{10}(NH)_2$ showed no luminescence since the smaller size of the coordination polyhedron impedes Eu^{2+} incorporation. However, intrigued by the natural solid solution series of micas like the phlogopite–aspidolite series $(K(Mg)_3AlSi_3O_{10}(F,OH)_2$-$NaMg_3AlSi_3O_{10}(OH)_2)$,[33] we have synthesized the compound $Mg_{1-x}Ca_xSi_3P_4N_{10}(NH)_2:Eu^{2+}$ ($x \approx 0.06$). Since the Ca content in this compound is below 0.5 at%, the Ca content was estimated by extrapolation of unit cell volumes between the end members $MgSi_3P_4N_{10}(NH)_2$ and $CaSi_3P_4N_{10}(NH)_2$. This compound showed the most red-shifted, narrow emission of the series at λ_{max} = 492 nm with an FWHM of 35 nm (1444 cm^{-1}).

Low-temperature emission spectra were recorded at 6 K (Figure S19), revealing the zero-phonon-line and giving insights into the vibrational modes of the layered crystal structure with an estimated phonon frequency of ca. 430 cm^{-1}. The rather high phonon-frequency may explain the strong thermal quenching (Figure S20).

Summarizing, based on the approach of employing NH_4F as a mineralizing agent, we were able to synthesize the first nitridic analogous mica through HP/HT syntheses.

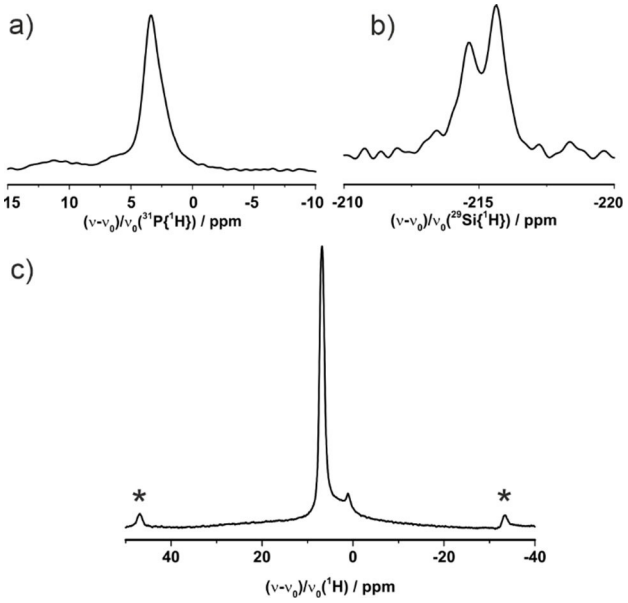

Figure 3. Solid-state NMR spectra of $CaSi_3P_4N_{10}(NH)_2$ at 20 kHz MAS speed. One signal in the $^{31}P\{1H\}$ (a) and two signals in the $^{29}Si\{1H\}$ (b) spectra agree with the structure model. c) ^1H NMR reveals one intense signal of the imide group of $CaSi_3P_4N_{10}(NH)_2$ while the weaker one belongs to $MgSi_3P_4N_{10}(NH)_2$. Rotation sidebands are marked with asterisks. Full spectra are provided in the Supporting Information.

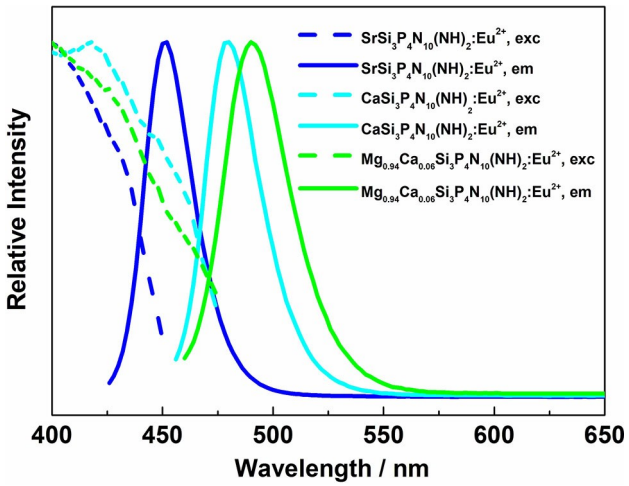

Figure 4. Emission spectra of $AESi_3P_4N_{10}(NH)_2$ (AE = $Mg_{0.94}Ca_{0.06}$, Ca, Sr) in solid lines. Emission maxima and FWHMs are: $Mg_{0.94}Ca_{0.06}$ 492 nm, 35 nm (1444 cm^{-1}), Ca 478 nm, 30 nm (1298 cm^{-1}) and Sr 451 nm, 26 nm (1300 cm^{-1}). Corresponding excitation spectra are shown with dashed lines.

Structure determination was performed by a combination of diffraction of microfocused synchrotron radiation on twinned crystallites, STEM-EDX and solid-state NMR. Eu^{2+}-doped samples showed narrow band emission from blue (451 nm) to cyan (492 nm). These findings represent the possibility of mimicking one of the most abundant and important aluminum silicates offering new scope for structural diversity and materials properties of nitrides. We expect that nitridic micas can act as model compounds to investigate the influence of aliovalent substitution of the cations and the influence of mixed anionic frameworks on physical properties such as luminescence and dielectric constants, e.g., by exchange of the imide group against OH groups or fluoride as this compositional range is already observed in natural micas.

Acknowledgements

Financial support by the Deutsche Forschungsgemeinschaft (DFG, SCHN 377/18-1, OE 513/6-1) is gratefully acknowledged. We thank Christian Minke for the acquisition of NMR data, SEM and EDX investigations. Furthermore, we are thankful for beamtime at the ESRF for the acquisition of microfocused single-crystal diffraction data (project CH-5663). Open Access funding enabled and organized by Projekt DEAL.

Conflict of Interest

The authors declare no conflict of interest.

Data Availability Statement

The data that support the findings of this study are available in the Supporting Information of this article.

Keywords: Electron microscopy · High-pressure · Mica · Nitride · Synchrotron

[1] O. Kazmina, E. Lebedeva, N. Mitina, A. Kuzmenko, *J. Coat. Technol. Res.* **2018**, *15*, 543–554.
[2] C. G. Low, Q. Zhang, *Small* **2012**, *8*, 2178–2183.
[3] M. Zhao, H. Liao, M. S. Molokeev, Y. Zhou, Q. Zhang, Q. Liu, Z. Xia, *Light: Sci. Appl.* **2019**, *8*, 38.
[4] L. Wang, R. J. Xie, T. Suehiro, T. Takeda, N. Hirosaki, *Chem. Rev.* **2018**, *118*, 1951–2009.
[5] M. Zeuner, S. Pagano, W. Schnick, *Angew. Chem. Int. Ed.* **2011**, *50*, 7754–7775; *Angew. Chem.* **2011**, *123*, 7898–7920.
[6] S. D. Kloß, W. Schnick, *Angew. Chem. Int. Ed.* **2019**, *58*, 7933–7944; *Angew. Chem.* **2019**, *131*, 8015–8027.
[7] S. Vogel, A. T. Buda, W. Schnick, *Angew. Chem. Int. Ed.* **2019**, *58*, 3398–3401; *Angew. Chem.* **2019**, *131*, 3436–3439.
[8] A. Zerr, G. Miehe, G. Serghiou, M. Schwarz, E. Kroke, R. Riedel, H. Fueß, P. Kroll, R. Boehler, *Nature* **1999**, *400*, 340–342.
[9] M. Schwarz, G. Miehe, A. Zerr, E. Kroke, B. T. Poe, H. Fuess, R. Riedel, *Adv. Mater.* **2000**, *12*, 883–887.
[10] W. Sinclair, A. E. Ringwood, *Nature* **1978**, *272*, 714–715.
[11] N. Kinomura, S. Kume, M. Koizumi, *Mineral. Mag.* **1975**, *40*, 401–404.
[12] L. Eisenburger, O. Oeckler, W. Schnick, *Chem. Eur. J.* **2021**, *27*, 4461–4465.
[13] L. Eisenburger, V. Weippert, O. Oeckler, W. Schnick, *Chem. Eur. J.* **2021**, *27*, 14184–14188.
[14] H. Huppertz, *Z. Kristallogr.* **2004**, *219*, 330–338.
[15] J. Wright, C. Giacobbe, M. Majkut, *Curr. Opin. Solid State Mater. Sci.* **2020**, *24*, 100818.
[16] F. Fahrnbauer, T. Rosenthal, T. Schmutzler, G. Wagner, G. B. M. Vaughan, J. P. Wright, O. Oeckler, *Angew. Chem. Int. Ed.* **2015**, *54*, 10020–10023; *Angew. Chem.* **2015**, *127*, 10158–10161.
[17] Deposition Number 2096670 contains the supplementary crystallographic data for this paper. These data are provided free of charge by the joint Cambridge Crystallographic Data Centre and Fachinformationszentrum Karlsruhe Access Structures service www.ccdc.cam.ac.uk/structures. Further details on the structure determination are given in the Supporting Information.
[18] E. H. Kisi, J. A. A. Crossley, S. Myhra, M. W. Barsoum, *J. Phys. Chem. Solids* **1998**, *59*, 1437–1443.
[19] M. Nespolo, G. Ferraris, H. Takeda, *Acta Crystallogr. Sect. A* **2000**, *56*, 132–148.
[20] H. Kalo, W. Milius, M. Bräu, J. Breu, *J. Solid State Chem.* **2013**, *198*, 57–64.
[21] M. Mallmann, C. Maak, R. Niklaus, W. Schnick, *Chem. Eur. J.* **2018**, *24*, 13963–13970.
[22] R. M. Hezen, C. W. Bunnnlvr, *Am. Mineral.* **1973**, *58*, 889–900.
[23] E. W. Radoslovich, *Acta Crystallogr.* **1960**, *13*, 919–932.
[24] M. Mallmann, S. Wendl, P. Strobel, P. J. Schmidt, W. Schnick, *Chem. Eur. J.* **2020**, *26*, 6257–6263.
[25] D. Baumann, W. Schnick, *Inorg. Chem.* **2014**, *53*, 7977–7982.
[26] E. Gnos, T. Armbruster, *Am. Mineral.* **2000**, *85*, 242–250.
[27] K. Nakamoto, *Infrared and Raman Spectra of Inorganic and Coordination Compounds*, Wiley, Hoboken, **2009**, p. 388.
[28] T. Sekine, M. Tansho, M. Kanzaki, *Appl. Phys. Lett.* **2001**, *78*, 3050–3051.
[29] N. E. Brese, M. O'Keeffe, *Acta Crystallogr. Sect. B* **1991**, *47*, 192–197.
[30] J. Tauc, R. Grigorovici, A. Vancu, *Phys. Status Solidi* **1966**, *15*, 627–637.
[31] E. A. Davis, N. F. Mott, *Philos. Mag.* **1970**, *22*, 903–922.
[32] S. Wendl, L. Eisenburger, M. Zipkat, D. Günther, J. P. Wright, P. J. Schmidt, O. Oeckler, W. Schnick, *Chem. Eur. J.* **2020**, *26*, 5010–5016.
[33] G. Tischendorf, H.-J. Förster, B. Gottesmann, M. Rieder, *Mineral. Mag.* **2007**, *71*, 285–320.

Manuscript received: November 3, 2021
Accepted manuscript online: December 2, 2021
Version of record online: December 10, 2021